Journal of Electronic Materials, Vol. 24, No. 10, 1995

Regular Issue Paper

The Effect of Soldering Process Variables on the Microstructure and Mechanical Properties of Eutectic Sn-Ag/Cu Solder Joints

WENGE YANG, LAWRENCE E. FELTON, and ROBERT W. MESSLER, JR.

Center for Integrated Electronics and Electronics Manufacturing and Department of Materials Science and Engineering, Rensselaer Polytechnic Institute, Troy, NY 12180-3590

Fundamental understanding of the relationship among process, microstructure, and mechanical properties is essential to solder alloy design, soldering process development, and joint reliability prediction and optimization. This research focused on the process-structure-property relationship in eutectic Sn-Ag/Cu solder joints. As a Pb-free alternative, eutectic Sn-Ag solder offers enhanced mechanical properties, good wettability on Cu and Cu alloys, and the potential for a broader range of application compared to eutectic Sn-Pb solder. The relationship between soldering process parameters (soldering temperature, reflow time, and cooling rate) and joint microstructure was studied systematically. Microhardness, tensile shear strength, and shear creep strength were measured and the relationship between the joint microstructures and mechanical properties was determined. Based on these results, low soldering temperatures, fast cooling rates, and short reflow times are suggested for producing joints with the best shear strength, ductility, and creep resistance.

Key words: Creep, microhardness, shear strength, Sn-Ag, solder, solder joint microstructure

INTRODUCTION

Eutectic Sn-Ag solder (96.5%Sn-3.5%Ag) is attractive to the electronics industry for several reasons. First, it is a candidate to replace eutectic and near-eutectic Sn-Pb solders which may be regulated due to the environmental hazards of Pb.[1-3] Second, since this solder has a melting point of 221°C (compared to 183°C for eutectic Sn-Pb), it may be suitable for higher temperature applications, such as under-the-hood electronics in automobiles.[4] Third, studies have shown that the shear strength, creep resistance, and thermomechanical fatigue behavior of bulk, eutectic Sn-Ag solders are among the best of all solders, making it possible to produce joints with superior reliability.[5-7] This interest has led to a number of studies of eutectic Sn-Ag solders.[8-12]

Understanding the relationship among process conditions, microstructure, and properties is important in applying any new material system. Soldering temperature, reflow time, and cooling rate are the major parameters in the soldering process, and many studies have shown the important influence each has on joint microstructure and mechanical behavior.[13-15]

As identified in previous research, eutectic Sn-Ag/Cu solder joints have three distinctive microstructural features:

- eutectic structure (Ag_3Sn intermetallic in essentially pure Sn matrix),
- η-Cu_6Sn_5 dendrites in the bulk solder due to copper dissolution from substrates, and
- Cu-Sn intermetallic layers at the joint interface.

Research on Pb-Sn solder has suggested that similar microstructural features such as coarseness of struc-

(Received January 23, 1995; revised June 27, 1995

Table I. Chemical Composition of Sn-Ag Eutectic Solder

	Sn	Ag		Bi	Cu	Fe	In	Ni	Pb	Sb
wt.%	96.46	3.49	ppm	82	11	57	43	65	36	157

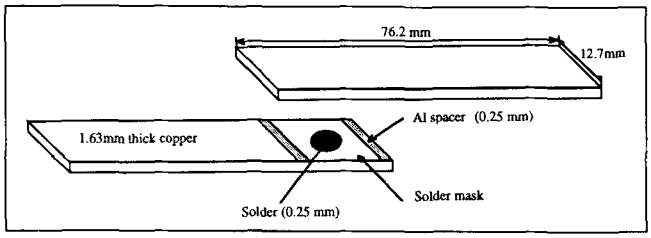

Fig. 1. Schematic diagram of lap shear specimen.

ture,[16] intermetallic whiskers in the bulk solder,[17] and intermetallic layers at interfaces have important effects on the joint shear strength, creep resistance, or fatigue properties.[18] This observation leads to the assumption that Sn-Ag solder joints will exhibit similar effects.

The research reported here systematically studied the influence of soldering temperature, reflow time, and cooling rate on the microstructure of eutectic Sn-Ag solder joints. It also explored the influence of each microstructural feature on the shear strength, ductility, and creep resistance of the joint. Based on this research, a process-structure-property relationship is presented for eutectic Sn-Ag/Cu solder joints. This relationship is analyzed to optimize the soldering process and joint reliability.

EXPERIMENTAL PROCEDURES

Eutectic Sn-Ag solder provided by Indium Corporation of America was used throughout this research. The chemical composition of the solder is shown in Table I. The solder was provided in the form of ingots, which were rolled and punched to 0.25 mm thick by 6 mm diameter preforms. Single-overlap shear specimens were prepared by soldering two pieces of commercially pure copper with the preforms. As shown in Fig. 1, the copper strips measured 76.2 × 12.7 × 1.63 mm, and an overlap of 30 mm was employed. The tarnish on the copper was removed by rinsing in the following series of solutions and solvents: 50% nitric acid; 2% sulfuric acid; running tap water; acetone; and, finally, methyl alcohol. Solder mask on the copper limited the spread of the solder during reflow. The mask was applied by positioning a circle of cellophane tape with a diameter of 6 mm on the copper. The tape and the exposed copper were then coated with the solder mask. The mask was dried for 10 min in an oven held at 100°C, then the cellophane tape was removed. The resulting bare copper circle on each piece was coated with an activated rosin flux. One solder preform was then placed on the bottom copper piece of the lap joint, and aluminum spacers of the same thickness as the preform were placed on either side of the solder preform to establish the joint thickness. The top piece of copper in the lap joint, similarly prepared, was then put in place.

Assembled lap shear specimens were reflow soldered individually in a temperature-controlled furnace. Three process variables—soldering temperature, reflow time, and cooling rate after soldering—were independently controlled to achieve variations in the joint microstructures. The baseline specimen, used as a reference for all comparisons, was soldered at 250°C for 20 min and cooled by quenching in room temperature water. The soldering time in actual production is much shorter than 20 min (typically, 1–2 min). The longer time used in this research is due to the large specimen size, which requires longer heating time to reach the solder melting temperature and equilibrate. It is also important to extend the time range to fully understand the time influence on joint microstructure.

The influence of each process variable on the joint microstructure was studied, in turn, by varying it while holding the remaining two variables at the baseline value. Specifically, the effect of soldering reflow temperature was studied by comparing specimens soldered at 350, 450, and 550°C with those soldered with the baseline conditions (i.e., 250°C, 20 min, water quenched). The influence of cooling rate was studied by comparing furnace-cooled and air-cooled specimens with the baseline. The effect of reflow time was studied by comparing specimens reflowed for 1000 min to specimens reflowed with the baseline conditions.

After soldering, lap joints were cut and mounted in epoxy to reveal their cross sections. Mounted specimens were polished and etched with 2% HNO_3-5% HCl-93% methyl alcohol solution for several seconds. The microstructures of the joints were evaluated using optical microscopy, scanning electron microscopy (SEM), and energy dispersive spectroscopy (EDS). Vicker's microhardness of the solder was also measured using a 10 gram load applied for 15 s.

The tensile shear strengths of the joints were measured in a screw driven Instron testing machine. Specimens were loaded and strained to failure at a cross head speed of 0.05 mm/s. The shear displacement in the joint was measured from the cross-head displacement of the testing machine. After mechanical testing, the fracture surfaces of ruptured joints were examined optically and by SEM.

Shear creep testing was done on a modified ATS split-furnace, lever-arm (10:1) testing machine. The bottom part of the lap shear specimen was fixed and the top part was pulled by the weight pan, while displacement was measured with a linear variable differential transformer (LVDT). The creep rate was measured at room temperature and at 158°C (87% of

the absolute melting temperature). All specimens were loaded until rupture, and the cross section of the joint was measured to determine the stress on the joint. The recorded data were transferred to a strain vs time curve to determine the steady-state strain rate. The time-to-rupture and total strain to rupture were also evaluated from the curves for each reflow condition at both room and elevated temperatures.

RESULTS AND DISCUSSION

The Effect of Soldering Process Parameters on Solder Joint Microstructure

Sn-Ag/Cu solder joints have three distinct microstructural features:

- The eutectic Sn-Ag constituent consisting of Ag_3Sn intermetallic dispersed throughout an essentially pure Sn matrix,
- The η-Cu_6Sn_5 dendrites formed in the bulk solder during solidification after Cu dissolves into the solder during reflow, and
- A continuous layer of η-Cu_6Sn_5 (and often a layer of η-Cu_3Sn as well in some conditions) at solder-copper interfaces formed while the solder is molten.[19]

Each of these microstructural features is identified in Fig. 2. The results presented in this section show how the soldering process variables including soldering temperature, reflow time, and cooling rate affect each of these features.

The influence of soldering temperature on joint microstructure is shown in Figs. 2a–2d. These joints were soldered at temperatures between 250 and 550°C. The reflow time was constant at 20 min, and all the joints were quenched in water after soldering. The micrographs show that increasing the soldering temperature increases both the amount and size of the η-Cu_6Sn_5 intermetallic dendrites in the bulk solder of the joint. This is the result of higher solubility and diffusivity of copper in the solder with increased temperature. Upon cooling, the dissolved Cu reacts with Sn to form the η-Cu_6Sn_5 dendrites.[19] Due to the higher Sn concentration, the dissolution of Cu into Sn-Ag solder is faster than that into eutectic Sn-Pb solders.[20] This leads to the conclusion that Sn-Ag joints will exhibit more dendrites than Sn-Pb joints soldered under similar conditions.

As expected, the thickness of the η-Cu_6Sn_5 intermetallic layer at the solder/Cu interface increases with soldering temperature. At the highest reflow temperature 550°C, a layer of ε–Cu_3Sn forms between the η-Cu_6Sn_5 and the Cu base metal. Note, also, that some voids formed with the formation of ε-Cu_3Sn intermetallic layer, probably from the Kirkendall effect in diffusion. A similar phenomena has been observed in Sn-Ag/Cu solder joints under other condi-

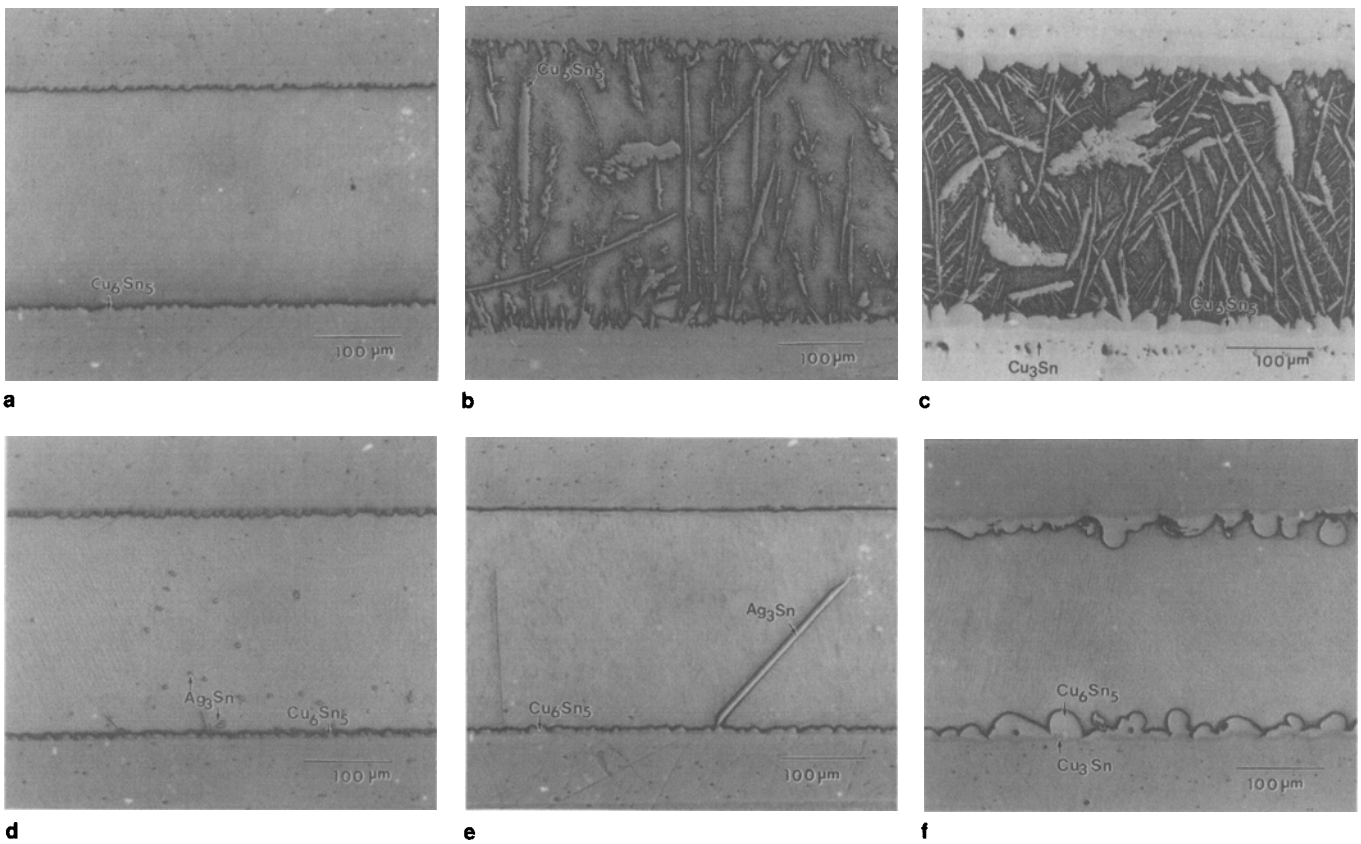

Fig. 2. The microstructure of Sn-Ag/Cu joints soldered with various process conditions. Soldering parameters (a) 250°C, 20 min, water quenched; (b) 350°C, 20 min, water quenched; (c) 450°C, 20 min, water quenched; (d) 550°C, 20 min, water quenched; (e) 250°C, 20 min, furnace cooled; and (f) 250°C, 1000 min, water quenched.

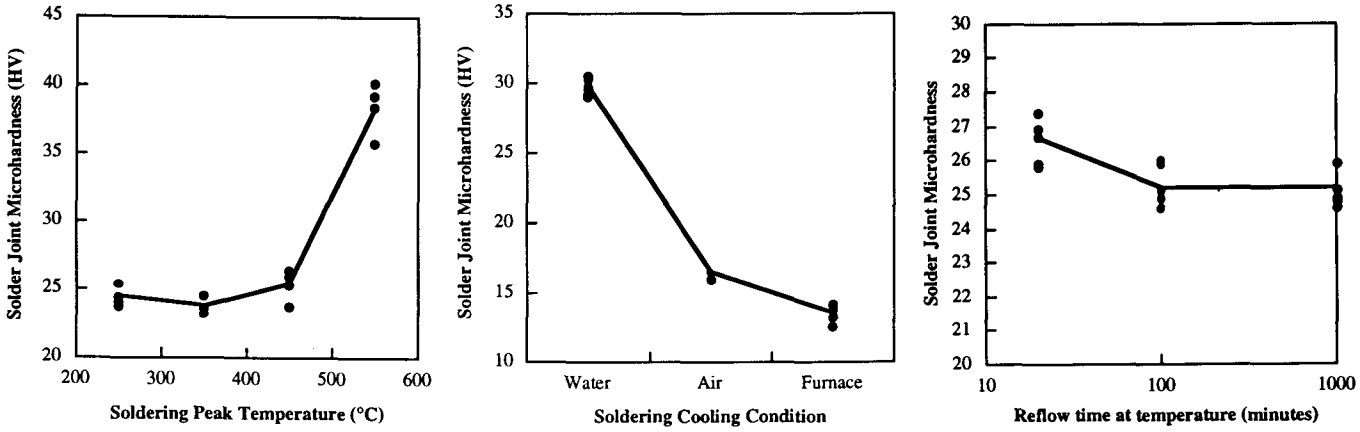

Fig. 3. The microhardness of Sn-Ag/Cu joints soldered with various process conditions: (a) the effect of temperature, (b) the effect of cooling method, and (c) the effect of soldering time.

tions.[11] The Ag_3Sn intermetallic phase is also present in these specimens in the form of fine precipitates, but the particles are too small to be resolved at the magnifications of these micrographs.

The influence of cooling rate following soldering on the joint microstructure is shown in Figs. 2a and 2e. Both joints were reflowed at 250°C for 20 min, but the joint in Fig. 2a was quenched in water, and the joint in Fig. 2e was cooled in the furnace. The micrographs show the size and morphology of the Ag_3Sn intermetallics change significantly as the cooling rate is changed. In the specimen subjected to the high cooling rate (water quenching), Ag_3Sn intermetallics are finely dispersed in the Sn matrix and can be seen only at high magnification (e.g., x4000) under the SEM. In the joint cooled in air (not shown), Ag_3Sn rods are visible at the solder/base metal interface. The rods grow perpendicular to the interface, reflecting the direction the solidification front movement during cooling. In the furnace-cooled specimen (Fig. 2e), larger, rod-like Ag_3Sn intermetallics are seen.

This finding is consistent with solidification theory and observations.[21,22] Due to the high volume fraction of Sn in eutectic Sn-Ag solder, the eutectic microstructure is formed with the Ag_3Sn particles or rods in the nearly pure Sn matrix. The slower cooling rate yields a coarser eutectic microstructure. Thus, the Ag_3Sn rods in the furnace-cooled specimen are larger than those in the air-cooled specimen. The high solidification rate obtained with water quenching suppressed the growth of the eutectic rods, yielding instead a finely dispersed spherical Ag_3Sn phase dispersed throughout the solder.

Figures 2a and 2f show the effect of reflow time on the joint microstructure. All the joints were reflowed at 250°C and water quenched, only the time at the reflow temperature was varied from 20 to 1000 min. Increased soldering time results in an increase in the thickness of the interfacial η-Cu_6Sn_5 layer, while other microstructural features remain the same. The same effect has been observed in Sn-Pb/Cu solder joints.[23,24]

These results show that, as expected, each of the principal microstructural features of Sn-Ag/Cu solder joints can be controlled by the soldering process parameters. In particular, the amount of η-Cu_6Sn_5 dendrites formed in the solder joints can be varied by adjusting the reflow temperature. The cooling rate controls the size and morphology of Ag_3Sn intermetallics. The reflow time (and temperature) determines the thickness of the η-Cu_6Sn_5 intermetallic layer at joint interfaces. This understanding of the relationship between key soldering process parameters and the joint microstructure enables a systematic study of the effect of joint microstructure on the mechanical properties of the solder joints.

Microhardness

As a first effort to assess the effects of changes in solder joint microstructure on mechanical behavior, the microhardness of the solder was measured at the overlap section of the joints. Figure 3a shows the effect of soldering temperature on joint hardness for constant reflow time and cooling rate. Since the hardness is measured at the bulk solder away from the joint interface, any changes would be due to the effects of the η-Cu_6Sn_5 dendrites, not the variations in the thickness of the interfacial η-Cu_6Sn_5 layer. The results show that, for temperatures less than 500°C, the microhardness of the solder joints is largely unaffected by the soldering temperature, indicating that the η-Cu_6Sn_5 dendrites do not significantly strengthen joints. This result is not surprising, given the large size of these dendrites. The joints soldered at 550°C have a much higher apparent hardness, due to the large volume of η-Cu_6Sn_5 dendrites. The volume fraction of dendrites was so high that it was impossible to make an indentation in a region of the bulk solder that did not also contain the dendrites. In fact, the high value reflects the high hardness of the intermetallic not the solder.

Figure 3b shows the effect of cooling rate on microhardness of joints soldered at 250°C for 20 min. The microhardness of the solder increases rapidly

with increased cooling rate. This result is consistent with the effects of cooling rate on the morphology of the Ag_3Sn intermetallics. During rapid cooling, the Ag_3Sn forms a dispersion of fine particles in the Sn matrix, while during slow cooling, large Ag_3Sn rods form. The smaller size and more uniform dispersion of these hard intermetallic particles should be more effective in strengthening the joint.

Figure 3c shows how reflow time affects the microhardness of joints soldered at 250°C and then water quenched. The data shows no significant change in the solder microhardness, indicating that the thicker intermetallic layers observed at joint interface due to the longer reflow time has little effect on the hardness or strength of the solder.

The Effect of Processing on Shear Strength

The results presented in the previous section show that the morphology of tbe Ag_3Sn intermetallics in the bulk of the solder predominately control the hardness of the solder joints. This finding suggests that other mechanical properties should be effected as well. In what follows, the effect of processing on the tensile shear and creep properties of Sn-Ag solder are reported. Since these tests are much more time consuming than hardness measurements, the number of processing conditions was reduced to four, as shown in Table II. The four conditions consisted of a baseline condition, designated A, and three others, B, C, and D, selected so as to systematically vary the three principal microstructural features one at a time. For example, condition B has a higher soldering temperature than condition A. The higher temperature will increase the amount of copper dissolution, thereby producing more η-Cu_6Sn_5 dendrites. Since the morphology of the Ag_3Sn phase depends mostly on the cooling rate, it will be the same in each joint. The thickness of the interfacial η-Cu_6Sn_5 layer increases with reflow temperature, but the fractography presented below shows that the joints failed in the bulk of the solder, not at the interface. Thus, any differences in the response of the joints are due to differences in the amount of the η-Cu_6Sn_5 dendrites.

Figure 4 shows the shear load-shear displacement curves for joints reflowed at the conditions detailed in Table II. The fracture surfaces of each of the joints is shown in Fig. 5. Comparing curve A to curve B in Fig. 4 shows that the increase in the amount of the η-Cu_6Sn_5 dendrites that results from soldering at a higher temperature only slightly increases the maximum shear strength in the joint, but considerably reduces the ductility. These large dendrites are ineffective in strengthening the joint but probably act as crack initiation sites, thereby reducing the joint ductility. Both joints failed in the solder, away from the interface. The fracture surfaces in Figs. 5a and 5b show that the joint with more dendrites failed in a more brittle manner.

The effect of cooling rate on shear deformation of the joints is observed by comparing curves A and C in Fig. 4. The furnace-cooled specimen shows a much

Table II. Reflow Conditions for the Mechanical Testing Specimens

	Solder Process Parameters		
Condition #	Soldering Temp.	Cooling Method	Solder Time (min)
A (baseline)	250°C	water	20
B	450°C	water	20
C	250°C	furnace	20
D	250°C	water	1000

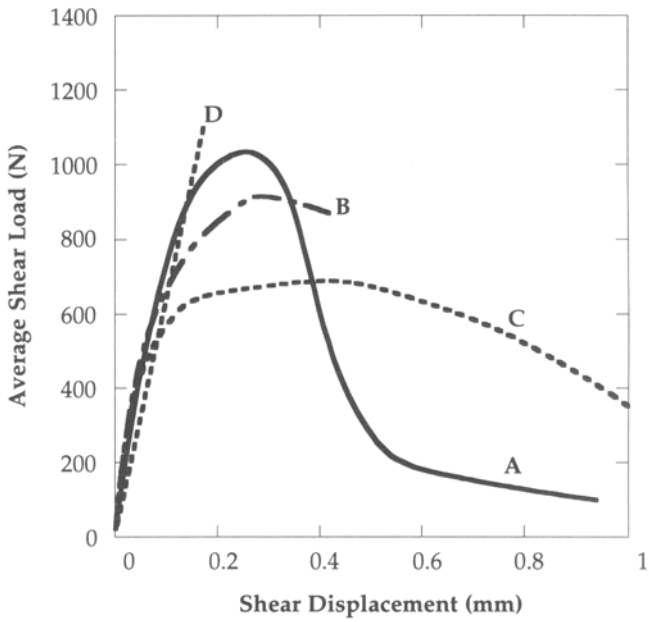

Fig. 4. Shear load vs shear displacement behavior of eutectic Sn-Ag/Cu joints soldered under various process conditions: A, baseline; B, higher peak temperature; C, slower cooling; and D, longer dwell time above liquidus.

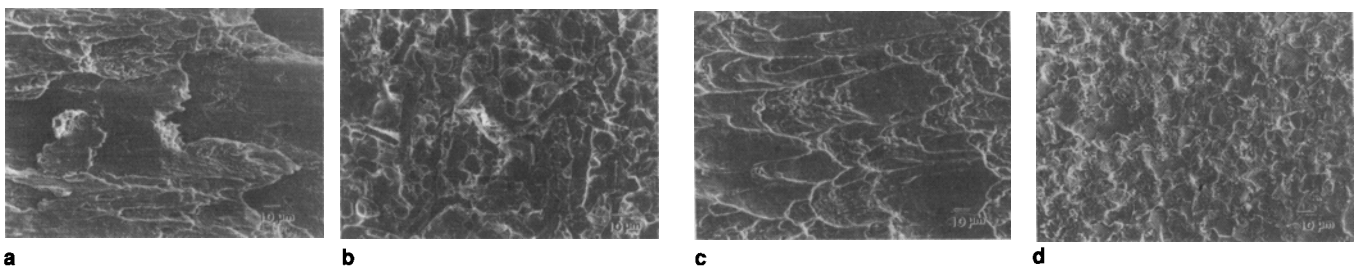

Fig. 5. The fracture surfaces of Sn-Ag/Cu joints soldered at various conditions and tested in shear: (a) baseline, (b) higher peak T, (c) slower cooling, and (d) longer dwell time (i.e., A,B,C, and D in Table II).

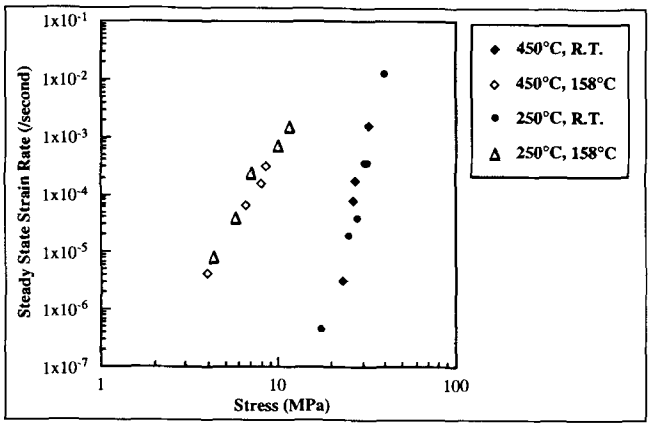

Fig. 6. Steady-state creep rate at room temperature and 158°C as a function of applied load of Sn-Ag/Cu joints soldered at conditions A and B in Table II.

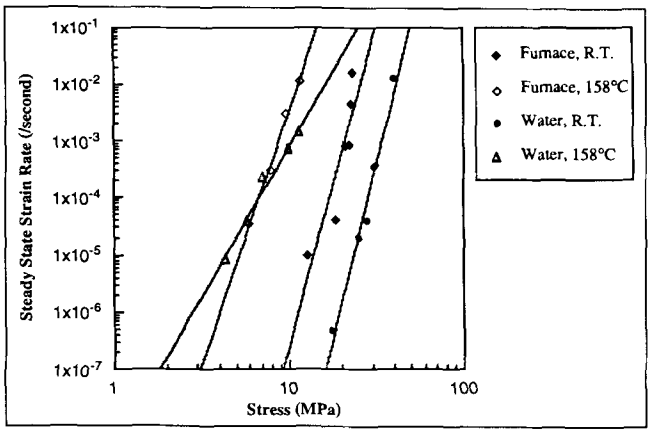

Fig. 7. Steady-state creep rate at room temperature and 158°C as a function of applied load of Sn-Ag/Cu joints soldered at conditions A and C in Table II.

lower maximum shear strength and greater ductility than the water-quenched specimen. This confirms the microstructure and microhardness results presented above that showed the morphology of Ag_3Sn intermetallics has a significant influence on the strength of the solder joints. Faster cooling generates finer dispersed Ag_3Sn particles in the Sn matrix which strengthen the solder, while slower cooling generates larger Ag_3Sn eutectic rods that have little strengthening effect. Figure 5c shows the fracture surface of the furnace-cooled specimen. Compared with the baseline specimen in Fig. 5a, more dimples were found in shear direction, indicating more ductile fracture, reflecting the measured ductility.

Comparing curves A and D in Fig. 4 shows the effect of soldering time on the joint shear load-shear displacement curves. Note the specimen soldered for the longer time exhibited no ductility. Joints soldered at these conditions exhibit a thick layer of interfacial intermetallic, and the fractograph in Fig. 5d shows brittle fracture through this layer.

The Effect of Processing on Creep Rate

The steady-state creep rate in shear was also measured for specimens soldered at the conditions detailed in Table II. Specimens were tested at room temperature and at 158°C (i.e., 87% homologous-temperature). Figure 6, a plot of steady-state creep rate vs stress, shows the influence of soldering temperature on creep behavior. For specimens tested at room temperature and 158°C, the data for both reflow temperatures (250 and 450°C) fall on the same lines. This result indicates that copper dissolution and resulting Cu_6Sn_5 dendrites do not affect the creep rate. The stress exponent is 12 at the room temperature and 5 at the higher temperature, indicating the creep mechanism changes with temperature.

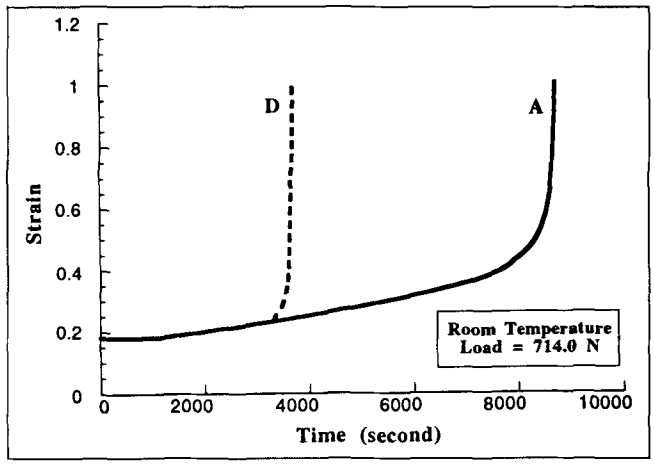

Fig. 8. Creep strain vs time for Sn-Ag/Cu joints soldered at conditions A and D in Table II.

The influence of the morphology of the Ag_3Sn phase on creep behavior is shown in Fig. 7. At room temperature, the steady-state creep rate of the furnace-cooled joints is almost three magnitudes larger than that of the water-quenched joints over the entire range of stresses tested. At 158°C, the furnace-cooled joints had a larger creep rate at high stresses, and a lower creep rate at low stresses. On the other hand, furnace-cooled joints have higher total strain-to-failure compared with water-quenched ones at both temperatures. These results show that the morphology of the Sn-Ag intermetallics plays the predominate role in determining the creep behavior of the solder joints. This phenomena is consistent with the results of the shear test.

The effect of reflow time on the steady-state creep rate was assessed by comparing the behavior of joints soldered for 20 and 1000 min. In both cases, the joints were soldered at 250°C and quenched in water after soldering. The results of these experiments, shown in Fig. 8, indicate that the steady-state creep rate was unaffected by reflow time. The strain at failure, however, decreased considerably for the longer reflow time. Analysis of the failed specimens showed that joints soldered for the longer time failed through the thick and brittle interfacial η-Cu_6Sn_5 layer, while those soldered at lower temperature failed in the bulk solder.

The results of the creep testing agree with the shear tests. Each microstructural feature contributes to the mechanical behavior of the joint. The presence of η-

Cu_6Sn_5 dendrites in the joints has little effect on the strength and creep rate of the solder, but reduces the joint ductility. Morphology and coarseness of the eutectic structure (or Ag_3Sn intermetallics) is the determining factor in strengthening of joints. Finely dispersed Ag_3Sn in the eutectic structure increases the shear strength as well as the creep resistance of the solder joint, while joints with a coarse eutectic structure exhibit greater ductility. Thick η-Cu_6Sn_5 intermetallic layers at interfaces drastically reduce the joint ductility and creep resistance by promoting failure through the intermetallic layers.

This study is a first step toward understanding the relationship between soldering process variables and the in-service reliability of Sn-Ag solder joints. The only effect of the presence of the η-Cu_6Sn_5 dendrites in the joints or the η-Cu_6Sn_5 layer at the solder/Cu interface is a reduction of ductility. This indicates that a soldering process should have low reflow temperatures and short reflow times to minimize the formation of these microstructural features. This result is in agreement with general industry practice of soldering for the shortest time at the lowest temperature that will ensure wetting at all the joints. The selection of the cooling rate after soldering, which determines the morphology and size of the Ag_3Sn phase, is not so straightforward. This is, in part, because the effect of the cooling rate on the creep rate depends on the application temperature and in part because it is difficult to predict how the creep rate relates to reliability. Clearly, experiments to assess the effects of microstructure on the thermomechanical fatigue properties of Sn-Ag solder joints are warranted.

Service temperatures for solder joints are high enough that the effects of aging on the joint microstructure and mechanical behavior must be considered. The thermomechanical cycling of joints during service will further accelerate the microstructural evolution. As a result, the as-soldered microstructure and mechanical properties of solder joints may not be stable during service. The microstructural evolution of eutectic Sn-Ag/Cu joints can be summarized as coarsening of the eutectic structure, coarsening of Cu-Sn intermetallics in the bulk solder, and the growth of intermetallic layers at interfaces.[11] According to the structure-property relationship drawn in this research, such microstructural evolution will result in a joint with lower shear strength, lower creep resistance, and more tendency toward brittle fracture at joint interfaces.

Due to testing difficulties, much of the data published concerning solder microstructure and mechanical properties has been based on bulk solder rather than actual solder joints. Disagreement has existed as to the use of bulk solder data in the design and analysis of actual solder joints. The results of this study indicate that it is important to use data gathered from actual solder joints because the microstructures of bulk solders differ from those of solder joints in significant ways. First, the bulk solders do not exhibit any Cu-Sn intermetallics, since these intermetallics form from the reaction of the solder with the base metal. These intermetallics, whether in the solder or at the solder/base metal interface, reduce the joints ductility. Secondly, large bulk specimens probably cool much more slowly than joints on real printed wire boards, greatly affecting the creep properties of the solders.

SUMMARY

This study detailed the relationship between soldering process parameters, microstructure and mechanical properties of eutectic Sn-Ag/Cu solder joints. The results showed that the microstructure and mechanical properties of the joints depended strongly on the process parameters.

For soldering process effects on joint microstructure, the amount and size of η-Cu_6Sn_5 dendrites in the joint increases with the soldering temperature due to increased dissolution of copper with increased temperature. The morphology of the Ag_3Sn intermetallic phase depends on the cooling rate; slow cooling rates yield eutectic rods in a Sn matrix, while faster cooling produces a dispersion of small Ag_3Sn spheres in the Sn matrix. The thickness of the interfacial Cu_6Sn_5 layer depends on the soldering time and temperature.

Measurements of the shear stress vs shear strain response of the joints revealed that the maximum strength of the joints depended primarily on the morphology of the Ag_3Sn intermetallic. Joints with small, spherical Ag_3Sn particles, produced by fast cooling, were stronger than slow cooled joints with Ag_3Sn eutectic rods. The peak strength of the joints did not depend on the amount of η-Cu_6Sn_5 dendrites, although the ductility of the joints decreased as the amount of dendrites increased. Increasing the thickness of the interfacial Cu_6Sn_5 joints dramatically reduced the ductility of the joints by promoting brittle failure through the layer.

The steady-state creep rate of the joints depended on microstructure in the same manner. The morphology of the Ag_3Sn phase had the greatest effect. Again, joints with small spherical Ag_3Sn particles exhibited the lowest creep rate. The amount of Cu_6Sn_5 dendrites did not affect the creep rate, although their presence reduced the joint ductility. Joints with thick Cu_6Sn_5 layers failed at very low strains by fracture through the intermetallic layer.

ACKNOWLEDGMENT

This study was part of the Electronic Manufacturing Program formerly in the Design and Manufacturing Institute (DMI) and now in the Center for Integrated Electronics and Electronics Manufacturing (CIEEM), Rensselaer Polytechnic Institute. This program is funded by AT&T, Boeing, Navy MANTECH, Northern Telecom, and Thomson Consumer Electronics. The authors thank the DMI and CIEEM for the support of this project. Dr. Don L. Millard is acknowledged for his technical support. We also thank Chris Raeder for his technical discussions and help, and Tarek Suwwan for his assistance in this research.

REFERENCES

1. S. Jin, *JOM* 45, 13 (1993).
2. L.E. Felton, C.H. Raeder, D.B. Knorr and C.H. Havasy, *Proc. 1992 Intl. Electronics Manu. Symp.* (1992), p. 300.
3. C. Melton, *Proc. 1993 IEEE Intl. Symp. Electronics and the Environment,* (1993), p. 94.
4. W.L. Winterbottom, *JOM* 45, 20 (1993).
5. W.J. Tomlinson and A. Fullylove, *J. Mater. Sci.* 27, 5777 (1992).
6. S.K. Kang and A.K. Sarkhel, *J. Electron. Mater.* 23, 701 (1994).
7. J.S. Hwang and R.M. Vargas, *Soldering & Surface Mount Techn.* 5, 38 (1990).
8. M. Harada and R. Satoh, *IEEE/CHMT* 13, 736 (1990).
9. J. Beuers and G. Ptashek, *Proc. IEEE/ISHM'92 Symp.* (1992), p. 120.
10. D. Shangguan and A. Achari, *Proc. 16th IEEE/CPMT Intl. Electronics Manu. Technology Symp.* (1994), p. 25.
11. W. Yang, L.E. Felton and R.W. Messler, Jr., *J. Electron. Mater.* 23, 765 (1994).
12. W. Yang, L.E. Felton and R.W. Messler, Jr., *Proc. Conf. Advanced Joining Technologies for New Materials II,* (1994).
13. M. McCormack, S. Jin and G.W. Kammlott, *Appl. Phys. Lett.* 64, 580 (1994).
14. F. Dirnfeld and J.J. Ramon, *Welding Journal* 69, 373s (1990).
15. M. Nylen and S. Norgren, *Soldering & Surface Mount Technology* 5, 15 (1990).
16. Z. Mei, J.W. Morris, Jr., M.C. Shine and T.S.E. Summers, *J. Electron. Mater.* 20, 599 (1991).
17. D. Frear, D. Grivas and J.W. Morris, Jr., *J. Electron. Mater.* 16, 181 (1987).
18. D. Frear, F.M. Hosking and P.T. Vianco, *Proc. Materials Developments in Microelectronic Packaging Conf.* (1991), p. 229.
19. L.E. Felton, K. Rajan, P.J. Ficalora and P. Singh, *Proc. Materials Developments in Microelectronic Packaging Conf.* (1991), p. 23.
20. W.G. Bader, *Welding Journal* 54, 370s (1975).
21. K. Fisher, *Fundamentals of Solidification* (Aedermannsdorf, Switzerland: Tech Trans Publications, 1986).
22. R.E. Reed-Hill, *Physical Metallurgy Principles,* 3rd Ed., (Boston: PWS-Kent Publishing Company, 1992).
23. A.J. Sunwoo, J.W. Morris, Jr. and G.K. Lucey, Jr., *Metall. Trans. A,* 23A, 1323 (1992).
24. E.K. Ohriner, *Welding Journal* 66, 191s (1987).